4 OAM x 4 WDM Optical Switching Based on an Innovative Integrated Tunable OAM Multiplexer

N. Zhang[(1)], M. Scaffardi[(2)], M. N. Malik[(2,3)], V. Toccafondo[(2)], C. Klitis[(1)], M. P. J. Lavery[(1)], G. Meloni[(2)], F. Fresi[(3)], E. Lazzeri[(3)], D. Marini[(1)] J. Zhu[(4)], X. Cai[(5)], S. Yu[(6)], L. Potì[(2)], G. Preve[(2)], A. Bogoni[(2,3)], M. Sorel[(1)]

(1) University of Glasgow, Oakfield Avenue, Glasgow G12 8LT, UK,
(2) CNIT, Via Moruzzi 1, 56124 Pisa, Italy
(3) Scuola Superiore Sant'Anna, Via Moruzzi 1, 56124 Pisa, Italy
(4) University of Bristol, University Walk, Bristol BS8 1TR, UK
(5) State Key Laboratory of Optoelectronic Materials and Technologies, Sun Yat-sen University, Guangzhou, China)
ning.zhang@glasgow.ac.uk

Abstract: A 4OAMx4WDM switching experiment has been carried out combining an innovative integrated tunable OAM multiplexer based on 4-concentric omega-shaped silicon waveguides and a refractive element-based OAM demultiplexer; operation is demonstrated up to 120Gb/s.
OCIS codes: (130.3120) Integrated optics devices; (130.4815) Optical switching devices

1. Introduction

The explosive growth of the Internet of Things requires a rapid increase of data center performance, which presents several challenging technological issues in terms of scalability of the current electrical interconnection networks [1]. Optical interconnection networks based on optical switching are regarded as an effective solution to overcome these issues [2]. The simultaneous use of different multiplexing domains, e.g. space and frequency, has been proposed for further enhancing the scalability and the total capacity [3]. Recently, we demonstrated the use of the orbital angular momentum (OAM) of light as an additional switching domain for a two-layer OAM-wavelength division multiplexing (WDM) interconnection network [4]. Not only OAM-based switching improves the scalability, but also the performance of the multilayer interconnection networks. In fact, OAM generation, multiplexing and demultiplexing can be carried out through compact and low power consuming devices. This makes the OAM switching energy-efficient and practical to implement. The standard technique to impress OAM onto a Gaussian beam is to use bulky passive devices such as spiral phase plates or active devices such as commercial spatial light modulators (SLMs) [5]. A reconfigurable 2x2 optical switch has already been demonstrated based on these devices[6]. However, integrated devices are more attractive for the small form factor, low-power consumption and fast tunability (i.e. tens of mW and μs timescale with thermal tuning) [7]. Integrated devices such as microrings with super-imposed grating structures8, circular grating couplers cascaded to star couplers [9] and hybrid 3D integrated circuits [10] have been demonstrated at component level. Microrings with super-imposed gratings have also been demonstrated in preliminary switching experiments where OAM and wavelength domains were not independently tunable [4].

In this paper we propose a new OAM multiplexer architecture based on concentric omega (Ω)-shaped waveguides, which is technologically simple and allows to independently map several WDM channels on multiplexed OAM beams. This device has been used in 4OAM x 4WDM switching experiments with 120Gb/s 16-quadrature amplitude modulation (QAM) and on-off keying (OOK) pseudo-random traffic. The switch has been implemented cascading a 4xΩ-shaped waveguide device used as OAM multiplexer and a compact passive refractive element-based device used as OAM demultiplexer [11]. This switch implementation represents a unique example of flexible two layer (OAM and wavelength) switch based on compact and low-power technologies, merging significant technological and system advances.
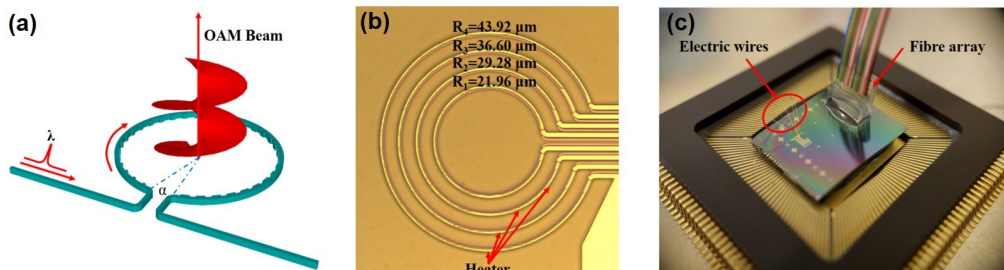

Fig. 1: (a) Schematic of a single Ω-shaped OAM beam emitter. (b) Optical microscope image of the four-layer Ω-shaped tunable OAM multiplexer (c) Packaged four-layer Ω-shaped tunable OAM multiplexer
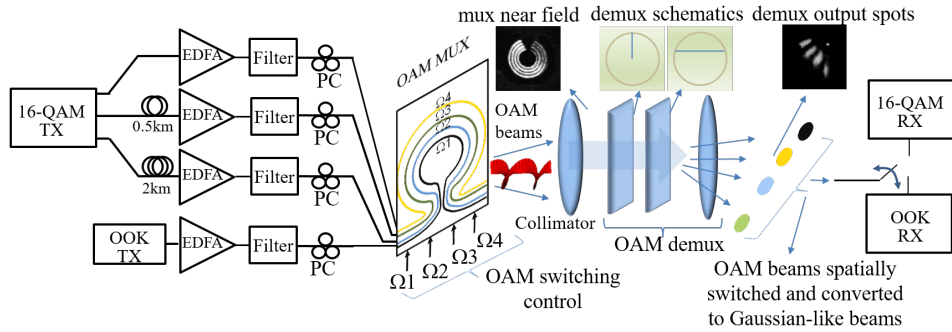
Fig. 2: (a) Experimental setup for OAM switching characterization. TX: transmitter; PC: polarization controller; RX: receiver. Insets: near-field intensity of the OAM mux, schematics of the two elements of the OAM demux, demux elongated spots.

The switch has been tested in all its critical configurations demonstrating penalty<1dB and a power consumption/Gb/s <0.6mW. Crosstalk measurement prove the device robustness and reliability.

2. Omega(Ω)-shaped tunable OAM multiplexer

Fig. 1 (a) illustrates the schematic of a single Ω-shaped OAM emitter, which consists of a ring geometry with an aperture α that enables the integration of multiple coaxial rings without any crossings between the bus waveguides. Second-order Bragg gratings are patterned on the inner sidewall of the Ω-shaped waveguide to scatter the confined whispering gallery modes (WGMs) to a vertically radiated OAM mode. The topological charge of the emitted OAM mode is l=(2π-α)Rn/λ-q, where n is the effective refractive index of the Ω-shaped waveguide and q is the grating number. The grating profile has been designed with an exponential increase along the waveguide propagation direction to keep the vertical emission uniform along the azimuthal direction and to decrease the potential penalty on the signal to noise ratio at the demultiplexer stage [12]. Fig. 1 (b) shows an optical microscope picture of the four-layer Ω-shaped OAM multiplexer. The four-layer Ω-shaped waveguides with radius ranging from 21.96μm to 43.92μm and out-coupling efficiency ranging from 15% to 20% are patterned coaxially to generate multiplexed OAM modes. The device is fabricated on a silicon-on-insulator (SOI) wafer with a 220nm-thick silicon core and a 2μm-thick buried oxide). Metallic heaters are defined in close proximity to each Ω-shaped waveguide to tune the radiated OAM mode independently with an efficiency of approximately 18mW per OAM mode. Fig. 1 (c) shows the silicon chip packaged in a ceramic chip carrier with bonded electric wires to tune the 4-concentric Ω-shaped OAM multiplexer and a pigtailed fiber array to couple the light into the OAM multiplexer. To demultiplex the OAM beams, a compact refractive element-based OAM sorter is used, which consists of two diffractive elements that can transform multiplexed OAM modes into a series of plane waves, each with a different phase tilt [11]. When focused using a lens, the tilted plane waves can be coupled to single mode fibers (SMF) placed in the focal plane of the lens, which enables an OAM demultiplexing process with high mode selectivity and low power consumption.

3. Experimental setup and results

A two-layer spatial switch based on the cascade of the integrated Ω-shaped OAM multiplexer (OAM mux) and the refractive element-based OAM demultiplexer (OAM demux) is built and tested according to the experimental setup shown in Fig. 2. The packaged integrated OAM multiplexer is vertically mounted to direct the OAM beams to the OAM demux, which spatially separates the incoming OAM beams depending on the OAM order. The performance of the switch is evaluated as a function of the order of the switched OAM mode for different wavelengths. A 16-QAM transmitter at 20 Gbaud generates a signal at wavelength 1549.9 and 1547.7nm fed into Ω4. The signal is switched by tuning the order of the emitted OAM mode from l=-3 to l=+1 by applying a proper voltage to the Ω4 control pad.

Fig. 3 shows the experimental results in terms of bit error rate (BER) versus the received optical signal to noise ratio (OSNR) that derived from different configurations. Fig. 3(a) depicts the case in which a single Omega (Ω4) was fed with two different wavelength (first 1547nm, then 1549nm), and was tuned to emit different OAM orders (l=-2,-1,0,+1 at 1547nm, and l=-3,-2,-1,0 for 1549nm). Fig 3(b) presents the results of a 4OAM x 4WDM switching demonstration: Ω4, Ω3 and Ω2 are fed with a 30 Gbaud 16QAM signal (120Gb/s) at 1555.7, 1548.5, and 1552.8nm, respectively, and Ω1 with a 30 Gbaud OOK signal at 1556.5nm, to evaluate the performance under mixed data traffic. Finally, the system was characterized in terms of crosstalk between adjacent Ω-shaped waveguides emitting subsequent OAM beam orders, and results are reported in Fig. 3(c). In Fig. 3(a) all the switched OAM modes have similar performance, i.e. OSNRs at BER 10-3 differ of <0.5dB. Since different wavelength channels can be

(a) Single Ω emitter: tuning over different OAM modes and wavelengths (single WDM channel-16QAM)

(b) OAM switch: four Ω emitters (4WDM channels-3x16QAM+1OOK)

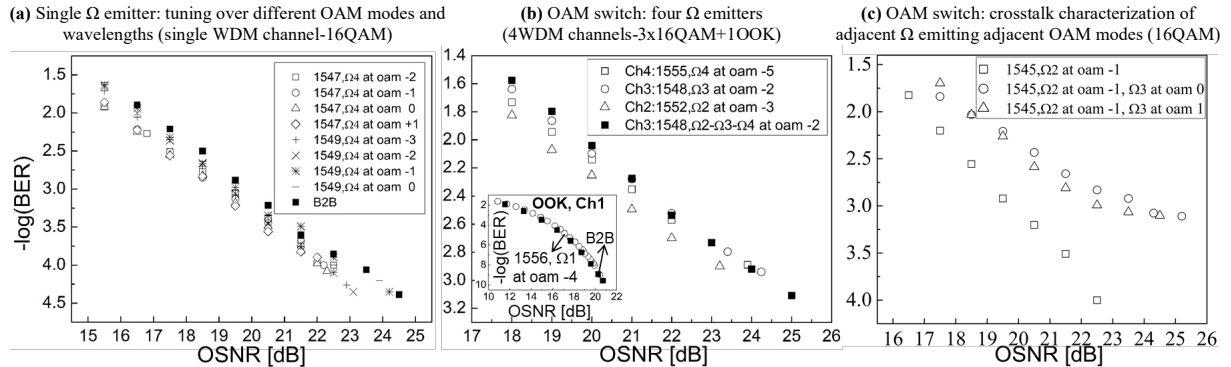**(c)** OAM switch: crosstalk characterization of adjacent Ω emitting adjacent OAM modes (16QAM)

Fig. 3: Experimental results. (a) BER vs switched OAM mode for single Ω-shaped emitter (2 WDM channels - 16QAM). (b) BER vs switched OAM mode for four Ω-shaped emitters (4 WDM channels - 3x16QAM+OOK). (c) Crosstalk characterization of the four Ω-shaped emitters

switched over the same set of OAM modes, the cascade of OAM mux and OAM demux can be exploited to implement a two-layer switch, where OAM and wavelength can be used as independent switching domains. In the mixed format (OOK and 16QAM) switching experiment, whose results are reported in Fig. 3(b), the chosen wavelengths correspond to the emission of integer OAM modes at room temperature. The signals are decorrelated by means of optical fiber spools. In a first switch configuration Ω4, Ω3, Ω2 and Ω1 emit an OAM beam of order l=-5, l=-2, l=-3 and l=-4 respectively. Then Ω4 and Ω2 are switched to l=-2, i.e. on the same OAM order of the beam emitted by Ω3. As shown in Fig. 3 (b), the performance is almost independent of the switching configuration, being the OSNR variation on the signal emitted by Ω3 negligible. The 16QAM penalty with respect to the back-to-back is <1dB. The inset shows that a very low penalty <0.2dB at BER 10-9 is measured on the OOK signal. Considering a maximum power consumption for each Ω emitter of 70mW, the switch total power consumption/Gb/s is <0.6mW for the tuning of the whole OAM multiplexer. In Fig. 3(c) the same 20Gbaud 16QAM signal at 1545.9nm was fed into Ω3 and Ω2 waveguides to measure the crosstalk. Three different measurements were taken, corresponding to the three BER curves depicted in Fig.3(c). In the first measurement the 1545.9nm signal was fed only in Ω2, which was tuned to emit l=-1 (squares in Fig.3 (c)). Then signal at Ω3 input was switched on and the waveguide was thermally controlled to emit l=0; BER was measured on the signal emitted by Ω2 waveguide on mode l=-1, showing the results depicted in Fig.3(c) in circles; finally Ω3 was set to emit mode l=1 and BER on mode l=-1, emitted by Ω2, were collected and are shown in triangles in Fig.3(c). A crosstalk penalty <4dB was measured.

4. Conclusions

An innovative integrated silicon tunable OAM multiplexer is fabricated, packaged and tested. By cascading the OAM multiplexer with a refractive element-based OAM demultiplexer, a two-layer switch is demonstrated exploiting both OAM and wavelength domain. The switch can operate with coherent polarization-multiplexed and amplitude-modulated traffic up to 30Gbaud with power consumption <0.6mW/Gb/s. Crosstalk measurements show the robustness and reliability of the switching system.

5. References

[1]J. Humphreys et al., "The impact of power and cooling on data center infrastructure," Market Research Report, IDC, 2006.
[2]H. Cho et al., "Power comparison between high-speed electrical and optical interconnects for interchip communication," JLT., 22, 2021, 2004.
[3]I. Cerutti et al., "Power and scalability analysis of multi-plane optical interconnection networks", IET Optoelect., 6, 192, 2012.
[4] M. Scaffardi et al., "A Silicon Microring Optical 2x2 Switch Exploiting Orbital Angular Momentum for Interconnection Networks up to 20Gbaud", J. Light. Tech., 2016.
[5]J. Wang et al., "Terabit free-space data transmission employing orbital angular momentum multiplexing", Nat. Photonics, v. 6, p. 488, 2012.
[6]N. Ahmed, et al., "Reconfigurable 2×2 orbital angular momentum based optical switching of 50-Gbaud QPSK channels", O. E., 22, 756, 2014.
[7]M. J. Strain et al., "Fast electrical switching of orbital angular momentum modes using ultra-compact integrated vortex emitters", Nat. Com., 5, 4856, 2014.
[8]Q. Xiao et al., "Generation of photonic orbital angular momentum superposition states using vortex beam emitters with superimposed gratings", Optics Express, 24, 3168, 2016.
[9]N. K. Fontaine et al., "Efficient multiplexing and demultiplexing of free-space orbital angular momentum using photonic integrated circuits", OFC, OTu1I.2, 2012.
[10]C. Quin et al., "Demonstration of Orbital Angular Momentum State Conversion using Two Hybrid 3D Photonic Integrated Circuits", OFC, Th4A, 2014.
[11] G. C. G. Berkhout, et al., "Efficient sorting of orbital angular momentum states of light," Physical Review Lett., 105, 153601, 2010.
[12] N. Zhang et al., "Manipulating optical vortices using integrated photonics", Front. Optoelectron. 9, 194, 2016.